

Notes

Electrospinning of Bovine Serum Albumin. Optimization and the Use for Production of Biosensors.

Tomasz Kowalczyk,^{*,†} Aleksandra Nowicka,[‡]
Danek Elbaum,[‡] and Tomasz A. Kowalewski[†]

Institute of Fundamental Technological Research, Polish Academy of Sciences (IPPT PAN), Swietokrzyska 21, Warszawa, 00-049, Poland, and Institute of Physics, Polish Academy of Sciences (IF PAN), al. Lotnikow 32/46, 02-668 Warsaw, Poland

Received April 17, 2008

Revised Manuscript Received May 6, 2008

Electrospinning of the globular protein, bovine serum albumin (BSA), was optimized to obtain proteinous fibers suitable as biosensors. It was shown that the as-spun protein preserves its native form, whereas solubility of the cross-linked in the ambient conditions BSA nanofibers evidently decreases. Insoluble BSA fibers can be easily modified to be used as two-dimensional biosensors. Here, we show the micro pH sensor obtained from the BSA fiber stained with a fluorescein derivative (FITC).

1. Introduction

Electrospinning is one major way to generate ultrafine fibers with diameters ranging from hundredths to tens of nanometers.^{1–6} Electrospun fibers can be produced of almost any synthetic or natural polymers, thus opening a plethora of biomedical applications.⁷ Significant progress has been achieved in electrospinning substrates for tissue growth,⁸ drugs and living cells encapsulation,⁹ and wound dressing,¹⁰ just to mention few biomedical applications. The coelectrospinning process of two or more materials opened very versatile methodology for encapsulation and release of bioactive agents. When water-resistant core material is used, an aqueous solution of a bioactive agent can be coelectrospun as the core–shell nanofiber.^{3–6} Recently, successful coaxial electrospinning of bovine serum albumin conjugated with fluorescein isothiocyanate has been reported by Greiner et al.³ and Zhang et al.⁶ It appeared that embedded bioactive agent remains not altered during the electrospinning process.

The present paper addresses major challenge of nanotechnology in biomedical diagnostics, namely biosensors enabling noninvasive imaging of living cell activity with nearly molecular resolution. Presently, specifically functionalized nanoparticles are used as biolabels. However, information gathered by such a sensor is limited to a small area only. Nanofibers could offer an interesting extension of this diagnostics methodology, permitting the analysis of the variation of the acquired signal along their length, that is, covering hundredths of micrometers. Proteins are good candidates for creating such sensors, as their

biologically active macromolecules can be easily introduced to the living environment and their unique binding properties simplify transport and anchoring procedures. Therefore, the focus of the present work is to develop protocols aimed to generate insoluble protein based nanofibers. According to our knowledge, it is the first reported approach to construct two-dimensional nanosensors from electrospun insoluble proteinous nanofibers.

Material selected for electrospinning was bovine serum albumin (BSA), a 68 kDa protein widely used in biotechnological applications as a blocking agent, tissue culture nutrient, and enzymatic stabilizer. BSA is a highly soluble protein (> 100 mg/mL), readily cross-linked by a variety of methods. It appeared that, when cross-linked in an ambient atmosphere, the electrospun BSA becomes insoluble, still maintaining its native structure. In addition, anticipating various potential applications of albumin-derived nanomaterial, we have prepared fluorescent nanofibers by covalently linking fluorescein isothiocyanate (FITC) to the fibrils made of BSA. We have demonstrated that the FITC-labeled BSA nanofiber is pH sensitive and, thus, could have potential application as a subtle pH sensor. The present report aims to provide a preliminary step in the development of protein based nanofibers with potential biomedical applicability.

2. Experimental Section

2.1. Materials. Poly(ethylene oxide) (PEO) of molecular weight 4×10^5 Da was purchased from Aldrich. Bovine serum albumin (BSA) of molecular weight 65×10^3 Da and fluorescein isothiocyanate (FITC) were purchased from Sigma Aldrich. Deionized water (DI; 0.5 MΩ cm), produced by Nano-Tech (Poland), was used as delivered without further purification. To avoid problems with molecular heterogeneity, all experiments were performed using the same BSA sample.

2.2. Equipment. A custom-made high voltage power supply based on a DC to DC converter (EMCO 4330) is the core of the experimental setup. It permits remote voltage adjustment in the range 0–33 kV, with a maximum current output of 0.3 mA. A separate sensitive (nanoampere range) amplifier was used to measure electric current carried by an electrospun nanofiber. A constant volume flow rate of the polymer solution is maintained using a syringe pump (Ascor S.A., AP12). A high-speed CMOS camera (PCO Imaging, pco.1200hs) was used to observe and record the electrospinning process. An epi-fluorescence microscope (Nikon, Eclipse E-50i) supplied with a high resolution CCD camera (Bassler, A102f), high pressure mercury lamp (Nikon, LHM 100C1), and FITC fluorescence filters (excitation band 465–490 nm, emission band 515–555 nm) was used to characterize optical characteristics of nanofibers and to evaluate their fluorescence. Surface geometry of the electrospun was characterized in air by an atomic force microscope (Veeco Inst., CP-II). A spectrophotometer Perkin-Elmer LS-35, supplied with a thermostatted cuvette, is used for evaluating protein denaturation and to quantify nanofibers solubility. Electrophoresis was conducted to verify the molecular structure of the electrospun protein, with polyacrylamide gel under nondenaturing conditions at 200 V (constant voltage) for 60 min and with an electrophoresis buffer of pH 8.8.

3. Results and Discussion

3.1. Electrospinning. Electrospinning was performed in a custom-made polycarbonate chamber of approximately 1 m³

* To whom correspondence should be addressed. E-mail: tomasz.kowalczyk@ippt.gov.pl.

[†] Institute of Fundamental Technological Research.

[‡] Institute of Physics.

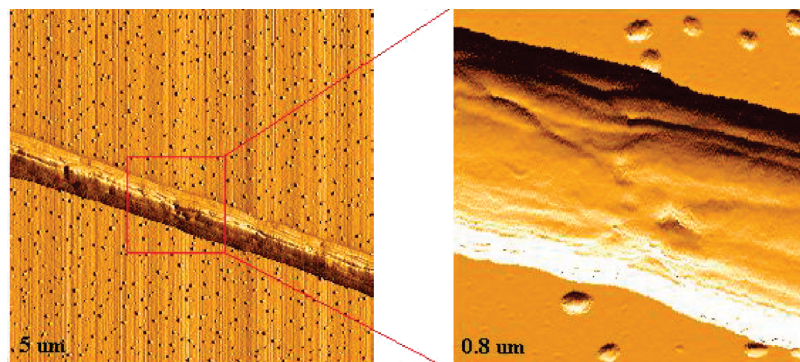


Figure 1. AFM picture of the BSA fiber reinforced with the addition of 15% PEO. The fiber width is nearly 400 nm. AFM height profile of this fiber indicates the thickness of the fiber to be only 73 nm. The scale corresponds to the image width (AFM scan size).

volume. The spinneret was made from a 2 mm long flat grounded syringe needle of 0.35 mm internal diameter (0.5 mm O.D.), mounted vertically on an electrically insulated stand. The spinneret needle was wired to a positive outlet of the high voltage power supply. A flat copper grid (310 mm × 240 mm) equipped with a small (75 mm × 80 mm × 50 mm) cage was used as a ground electrode, as described in detail by Kowalewski et al.¹¹ The electrospun fibers were collected on microscope cover glass slides (0.1 × 24 × 60 mm, Roth, Karlsruhe) positioned on the copper cage. The capillary needle spinneret was connected through PTFE tubing to a plastic syringe filled with a spinning solution. A constant volume flow rate was maintained using the syringe pump.

Our preliminary studies indicated that BSA solutions made by dissolving it in DI water at concentrations of 2–15 wt % would not generate a fibrous structure at any input voltage of electrospinning. Several studies have shown^{12,13} that one way to evade such a limitation is to blend the natural polymer solution with a miscible hydrophilic synthetic polymer, such as PEO. It is one of the most extensively studied of all water-soluble synthetic polymers, both for its biocompatibility and electrospinning ability at a wide range of concentrations.¹⁴ Hence, to make BSA solution spinnable, PEO was used as the supporting polymer.

Although electrospinning was demonstrated to occur for a large variety of polymeric solutions, polymer melts, and even for highly viscous liquids (e.g., glycerol¹¹), in practice, a stable process can be accomplished only after a long and tedious “*trial and error*” procedure of searching for the optimal process parameters. It is because the electrospinning process is affected by a large number of parameters and processing variables and their influence on the process is still not fully understood. These parameters include viscosity, surface tension, concentration, polymer molecular weight, viscoelasticity, and dielectric properties of the spinning solution. The process parameters, such as feed rate of the syringe pump, the electric potential, geometry of the electric field, distance between the spinneret, the ground electrode, and also the temperature and humidity of the environment, are known factors influencing reproducibility of the electrospinning.¹⁵ There are several possible routes to optimize the selected process. One of them, recently described by Kowalewski et al.,¹¹ is based on evaluating the geometry of fiber coils observed during the electrospinning process. High speed images of the electrospinning jet indicate that electrospinning typically results in bending instability of the jet beginning at some distance from the spinneret. Initially the jet forms a nearly straight line about 1 to 5 cm long after it bends in a complex spiraling path encircled by a conical envelope. The key geometrical parameters of the process, that is, the spiral

envelope angle and the length of the straight jet segment were obtained from the high-speed camera images. Their dependence on applied voltage, flow rate, spinneret–ground electrode distance, and solution composition was evaluated and correlated with microscopic images of the electrospun nanofibers. Applying this approach, the optimal process parameters were evaluated for our experimental configuration. The distance between electrode and target was set to 150 mm. The main variables changed were the applied voltage (from 5 kV up to 30 kV), PEO/BSA ratio (from 0 to 50%), concentration of polymers in the spinning solution (from 7 to 15%), and flow rate (to match the varied electric potential). Finally, the process parameters found to be optimal for our configuration were the flow rate (0.2 mL/h), electric potential (15 kV), and the corresponding current (0.12 μ A). The optimal percentage of polymers was found to be 85% of BSA and 15% of PEO (wt). The optimal concentration of the spinning solution was found to be 8.7% wt of the BSA and PEO polymers mixture. The environmental conditions for most experimental runs were ambient temperature, 22 °C, and humidity, 30%.

After stipulating optimal experimental conditions, over 30 separate samples of electrospun nanofibers were collected on the microscope cover glass slides. Each sample was collected during a defined time interval of 120 s to obtain reproducible density of the collected electrospun mat. The collected amount was selected to obtain a relatively sparse web-like matrix, easy to analyze under the optical microscope. A total of 1 order of magnitude longer collection periods were applied to prepare samples used for solubility tests of the nanofibers.

Owing to the small size of the nanofibers, their thickness cannot be estimated under optical microscope. Hence, the two-dimensional structure of the single fiber was measured using atomic force microscope (AFM). Figure 1 illustrates reconstructed image of the electrospun BSA/PEO nanofiber. It was found that the diameter of collected fibers was in the range of a few hundreds of nanometers of the same material. It is worth noting a noncircular cross-section of the recorded fiber. The AFM images indicate rather a ribbon-like shape of the fiber with 73 nm thickness and 400 nm width. This phenomena could occur when the charged jet was not dry enough prior to its deposition on the target. It is also possible that the collapsed skin-core fibers morphology^{5,16} resulted in their flattening by electrostatic and impact stresses. In fact, several analyzed AFM images indicated fiber flattening ratio even as high as 1:10. However, we have to admit that due to the limited access to the AFM we are not able to attest that the ribbon-like structure is typical for the process we used.

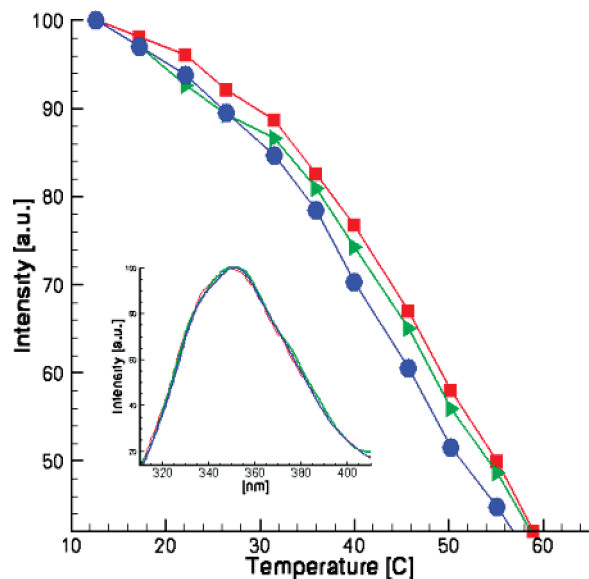


Figure 2. Temperature denaturation profiles of native BSA (squares) and BSA/PEO blend before spinning (circles) and after electrospinning (triangles), measured by monitoring fluorescence intensity of tryptophan at 348 nm. Inset shows overlapping emission spectra of tryptophan obtained for all three samples.

3.2. Characterization of Electrospun BSA/PEO Blend.

Conversion of native protein into nanofibers through electrospinning involves significant electrostatic and mechanical stresses executed on the polymer structure.¹⁷ It may potentially affect the biological material, altering its biological activity or leading to its denaturation. To evaluate this effect, the freshly prepared electrospun fibers were dissolved in deionized water and compared with the solution of native BSA. Two test runs were performed to assess the potential change of the BSA molecular structure: electrophoresis and fluorescence.

The electrophoresis test was carried out under non-denaturing conditions at pH 8.8 and temperature 25 °C. The position of the protein zone was generally determined by inspection of three major mobility peaks. The electrophoretic mobility of electrospun BSA proved to be the same as that of the BSA taken directly from the flask (data not shown). Hence, it could be concluded that the electrospinning procedure does not significantly change the protein molecular conformation, which could result in the alteration of the protein quaternary structure.

In the second test, we evaluated the effect of electrospinning on the protein intrinsic fluorescence of aromatic amino acid residues before and after the electrospinning process. In addition, we measured the temperature denaturation profiles of BSA fibers resulting from electrospinning, BSA/PEO blend before the spinning, and native BSA (Figure 2). All experiments were performed for buffered solutions of pH 7.3 (PBS). We selected 295 nm (excitation wavelength) to maximize tryptophan fluorescence at 348 nm (emission maximum). Our results, based on the temperature denaturation profiles and fluorescence emission spectra, provide no evidence of any significant alteration of BSA secondary structure induced by PEO alone or by an electrospinning process in the presence of the PEO core material. Our observation was based on similar emission profiles of BSA before and after electrospinning and undistinguishable thermal denaturation profiles of the BSA before and after the above-mentioned process. Analogue observations were made applying 280 nm excitation wavelength, which resulted in tyrosine and tryptophan emission. We have concluded that electrospinning does not denature albumin. Therefore, it was anticipated that

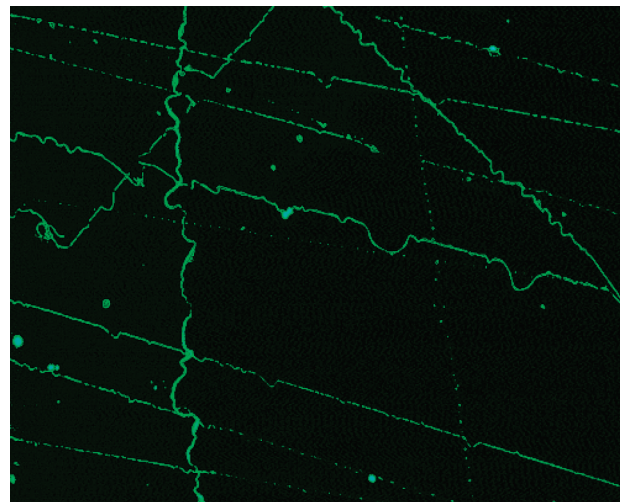


Figure 3. FITC stained BSA electrospun nanofibers observed under fluorescence microscope. Image length corresponds to 0.18 mm.

the electrospun nanofibers can be used for the preparation/anchoring BSA-based proteinous systems.

3.3. Fabricating Insoluble BSA Nanofiber. Freshly collected BSA/PEO electrospun nanofibers were easily soluble in water. It was found that nanofibers collected on the glass slide completely dissolved in DI water within a few seconds. However, after the nanofibers were aged for about two weeks in the ambient conditions, their proteinous part became insoluble and stuck to the glass substrate. The glass slit with the obtained nanofibers was kept in water for over one week and periodically observed under the microscope. Evidently, there were no visible changes of fiber geometry. To quantify solubility of the matured BSA fibers, the fluorescence of solvent was measured. For this purpose, a small sample of the matured BSA nanofibers was immersed in 25 mL of PBS buffered water (pH 7.4) and fluorescence of the solution probes was measured for a period of two weeks. The sample was kept in a bath with a constant temperature of 37 °C. After two weeks, the nondissolved fibers could be observed under the optical microscope. In all solvent samples taken during this period we could not detect tryptophan fluorescence emission (measured at 345 nm, excitation at 295 nm), indicating that BSA remained in the fibers. This test gives us confidence that BSA nanofibers will remain stable in the typical biological (water) environment long enough to be useful for diagnostic purposes.

The insoluble BSA nanofibers after appropriate preparation can be used as two-dimensional biosensors. One of the simplest modifications is staining nanofibers with fluorescent dyes. For this purpose the matured and washed proteinous fibers were subsequently immersed in 0.02% (wt) FITC solution and left at the room temperature for 24 h. The FITC tagged nanofibers were subsequently rinsed several times in the deionized water. The excess of the tagging agent was completely washed out leaving stable FITC stained nanofibers. Figure 3 illustrates the micrograph of FITC stained BSA nanofibers observed under fluorescent microscope. Despite the maturing process and washing in water, the typical pattern of several of the parallel and crossed nanofibers was well preserved on the glass slide (Figure 3). We assumed that during this procedure the PEO component of the fibers could be washed out by water leaving tagged insoluble BSA–FITC conjugated nanofiber.

The fluorescent proteinous fibers can be used to visualize the scaffold structure, its interaction with biological material in cell cultures, to control coating by wound dressing, and also to

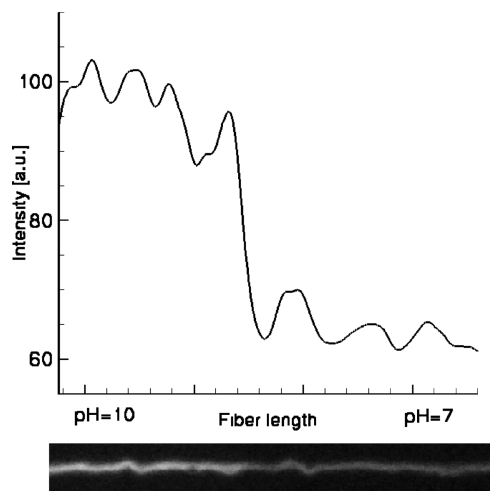


Figure 4. Effect of pH on the fluorescence of a single FITC-BSA nanofiber observed under a microscope. The left side of the fiber was exposed to an alkaline solution (pH = 10). The graph (top) shows the relative change of the fluorescence intensity; (bottom) the analyzed fiber under fluorescence microscope, where the image length corresponds to 80 μm .

construct fluorescent sensors. For example, it appears possible to construct FRET (fluorescence resonance energy transfer) sensors by collecting complementary stained nanofibrous material on the glass slide. Interrogating under the optical microscope the collecting glass, it is relatively easy to select fibers crossing each other and remaining close enough to permit resonance energy transfer. The small FRET-activated crossing area of two fluorescent fibers becomes sensitive to its environment, creating a confined chemical sensor. Our preliminary experiments seem to confirm this potential applicability of fluorescent nanofibers.

Monitoring of the intracellular pH in living cells is of high importance. Besides direct electrical methods, the intracellular pH can be measured by means of pH-sensitive fluorescent probes. The probe introduced into the cytoplasm or the cell membrane changes its fluorescence characteristics depending on a proton concentration and, consequently, reports on the pH of its environment. Here we demonstrate that the FITC-tagged insoluble BSA nanofiber can be used as a local pH sensor. Figure 4 (bottom) shows the fluorescent BSA nanofiber observed under the fluorescent microscope. The left part of the fiber is immersed in an alkaline buffer (pH = 10), whereas the right part remains in the neutral environment. The increased intensity of the fiber fluorescence in the alkaline environment can be easily noticed even without a sophisticated apparatus. The fluorescence measurements performed, for example, for fibers

attached to a cell membrane or incorporated to a cell culture may be used for monitoring their biological activity.

4. Conclusions

This study reports the feasibility and optimization of the electrospinning of the globular, highly soluble, naturally occurring BSA protein into insoluble fibrillar structures. It was shown that electrospun fibers preserve the molecular structure of the native protein. Hence, it can be assumed that biological properties of BSA nanofibers are still maintained. The result opens new possibilities for applying insoluble proteinous fibrils as two-dimensional biosensors, as well as a new scaffold material for cell growth.

Acknowledgment. This work was supported by Polish Ministry of Science Grant No. N508 031 31/1740. The authors thank Diana Lamparska for her invaluable help in experimental work. We also appreciate the help of Andrzej Szczepankiewicz, Slawomir Blonski, Piotr Korczyk, and Remigiusz Worch for fiber analysis and interpretation of the results.

References and Notes

- (1) Burger, C.; Hsiao, B. S.; Chu, B. *Annu. Rev. Mater. Res.* **2006**, *36*, 333–368.
- (2) Reneker, D. H.; Yarin, A. L.; Zussman, E.; Xu, H. *Adv. Appl. Mech.* **2007**, *41*, 43–195.
- (3) Greiner, A.; Wendorff, J. H.; Yarin, A. L.; Zussman, E. *Appl. Microbiol. Biotechnol.* **2006**, *71*, 387–393.
- (4) Dror, Y.; Salalha, W.; Avrahami, R.; Zussman, E.; Yarin, A. L.; Dersch, R.; Greiner, A.; Wendorff, J. H. *Small* **2007**, *3*, 1064–1073.
- (5) Yarin, A. L.; Zussman, E.; Wendorff, J. H.; Greiner, A. *J. Mater. Chem.* **2007**, *17*, 2585–2599.
- (6) Zhang, Y. Z.; Wang, X.; Feng, Y.; Li, J.; Lim, C. T.; Ramakrishna, S. *Biomacromolecules* **2006**, *7*, 1049–1057.
- (7) Vengopal, J.; Zhang, Y. Z.; Ramakrishna, S. *J. Nanoeng. Nanosyst.* **2005**, *218*, 35–45.
- (8) Arumuganathar, S.; Jayashinghe, S. N. *Biomacromolecules* **2008**, *9*, 759–766.
- (9) Gensheimer, M.; Becker, M.; Brandis-Heep, A.; Wendorff, J. H.; Thauer, R. K.; Greiner, A. *Adv. Mater.* **2007**, *19*, 2480–2482.
- (10) Zhou, Y.; Yang, D.; Chen, X.; Xu, Q.; Lu, F.; Nie, J. *Biomacromolecules* **2008**, *9*, 349–354.
- (11) Kowalewski, T. A.; Blonski, S.; Barral, S. *Bull. Pol. Acad. Sci.: Tech. Sci.* **2005**, *53*, 385–394.
- (12) Zhang, Y. Z.; Su, B.; Ramakrishna, S.; Lim, C. T. *Biomacromolecules* **2008**, *9*, 136–141.
- (13) Bhattacharai, N.; Edmondson, D.; Veiseh, O.; Matsen, F. A.; Zhang, M. *Biomaterials* **2005**, *26*, 6176–6184.
- (14) Theron, S.A.; Zussman, E.; Yarin, A. L. *Polymer* **2004**, *45*, 2017–2030.
- (15) Thompson, C. J.; Chase, G. G.; Yarin, A. L.; Reneker, D. H. *Polymer* **2007**, *48*, 6913–6922.
- (16) Dayal, P.; Kyu, T. *Phys. Fluids* **2007**, *19*, 1011061–9.
- (17) Reznik, S. N.; Yarin, A. L.; Zussman, E.; Bercovici, L. *Phys. Fluids* **2006**, *18*, 062101–13.

BM800421S